
# The IL-9R/Arg1 pathway promotes polyamine metabolism in human airway macrophages

Wenwu Zhang, MD PhD, In Su Cheon, PhD, Abigail Pajulas, PhD, Anthony L. Sinn, BS LAT, Maya Shraddha Krishnan, PhD, Jilu Zhang, PhD, Ahmed M. Abdelaal, PhD, Xin Liu, Kaitlyn G. Jackson, PhD, Jayden Zhang, Karen E. Pollok, PhD, Kirsten M. Kloepfer, MD, Homer L. Twigg, III, MD, Benjamin Gaston, MD, W. Gerald Teague, MD, Jie Sun, PhD, Mark H. Kaplan, PhD

PII: S0091-6749(26)00625-1

DOI: https://doi.org/10.1016/j.jaci.2026.08.016

Reference: YMAI 17305

To appear in: *The Journal of Allergy and Clinical Immunology*

Received Date: 6 February 2026

Revised Date: 19 July 2026

Accepted Date: 20 August 2026

Please cite this article as: Zhang W, Cheon IS, Pajulas A, Sinn AL, Krishnan MS, Zhang J, Abdelaal AM, Liu X, Jackson KG, Zhang J, Pollok KE, Kloepfer KM, Twigg III HL, Gaston B, Teague WG, Sun J, Kaplan MH, The IL-9R/Arg1 pathway promotes polyamine metabolism in human airway macrophages, *The Journal of Allergy and Clinical Immunology* (2026), doi: https://doi.org/10.1016/j.jaci.2026.08.016.

# The IL-9R/Arg1 pathway promotes polyamine metabolism in human airway macrophages

Wenwu Zhang MD PhD[1], In Su Cheon PhD[2], Abigail Pajulas PhD[1], Anthony L Sinn BS LAT[3], Maya Shraddha Krishnan PhD[1], Jilu Zhang PhD[1], Ahmed M. Abdelaal PhD[1,7], Xin Liu[1], Kaitlyn G Jackson PhD[1], Jayden Zhang[1], Karen E. Pollok PhD[3,4], Kirsten M. Kloepfer MD[4], Homer L. Twigg III MD[5], Benjamin Gaston MD[4], W. Gerald Teague MD[6], Jie Sun PhD[2], Mark H Kaplan PhD[1,3,4§]

1. Department of Microbiology & Immunology, Indiana University School Medicine, Indianapolis IN.

2. Beirne B. Carter Center for Immunology Research, Division of Infectious Diseases and International Health, Department of Medicine, University of Virginia School of Medicine, Charlottesville VA.

3. IU Simon Comprehensive Cancer Center, Indiana University School Medicine, Indianapolis IN.

4. Department of Pediatrics, Indiana University School Medicine, Indianapolis IN.

5. Division of Pulmonary, Critical Care, Sleep, and Occupation Medicine, Indiana University Medical Center, Indianapolis, Indiana, 46202

6. Child Health Research Center, Department of Pediatrics, University of Virginia School of Medicine, Charlottesville, VA.

7. Department of Zoology, Faculty of Science, Zagazig University, Zagazig Egypt, 44519

ABSTRACT

Background: Lung macrophages are central regulators of inflammatory responses in the airways and lung parenchyma. Macrophages function as conduits for cytokine function in the inflammatory milieu. We previously demonstrated that IL-9-responsive macrophages are essential for allergic lung inflammation in an arginase 1 (Arg1) pathway.

Objective: Define the IL-9/Arg1/polyamine pathway in human macrophages from model systems and asthmatic patient samples.

Methods: Using humanized NSG-Quad mice treated with intranasal IL-9 and patient bronchoalveolar lavage (BAL) samples, we evaluated macrophage phenotypes via flow cytometry, bulk RNA sequencing, and metabolic assays.

Results: Two distinct human lung macrophage populations were defined by the expression of CD43. IL-9 promoted the expansion of IL-9R+/Arg1+ CD43- macrophages in humanized mice. In parallel, greater proportions of IL-9R+/Arg1+ CD43- macrophages were observed in asthmatic patient BAL samples compared with healthy control patients. Higher concentrations of polyamines, downstream metabolites of Arg1 function, were detected in BAL of IL-9-treated humanized mice. There were increased concentrations of polyamines in asthmatic patient BAL, compared to control samples, and concentrations were positively correlated to BAL IL-9 concentration and increases of IL-9R+ and Arg1+ CD43- macrophages.

Conclusions: IL-9-responsive CD206+ CD43- macrophages alter the metabolites present in the lung milieu. These data provide evidence for an IL-9R/Arg1/polyamine lung macrophage axis that is active in asthma patients.

Key Findings:

- The CD43- lung macrophage subset acts as a primary target for IL-9 signaling in the airway.
- IL-9 upregulates its own receptor (IL-9R) and Arginase-1 (Arg1) in CD43- macrophages, promoting an increase in downstream airway polyamine metabolism and tissue remodeling pathways
- Therapeutic targeting or antibody blockade of the IL-9/macrophage/polyamine axis may offer a precision therapeutic avenue for subsets of asthma patients displaying a high IL-9 phenotype.

Capsule Summary

This study demonstrates that IL-9 expands a distinct population of CD43- airway macrophages that promote arginase-dependent polyamine production, altering the local metabolic environment in asthmatic adult and pediatric lungs.

KEYWORDS

Asthma; Allergic lung inflammation; Cytokine signaling; Macrophage; IL-9; Arginase; Polyamine; CD43.

Abbreviations list

AM, alveolar macrophage; Arg1, arginase 1; BAL, bronchoalveolar lavage; BALF, bronchoalveolar lavage fluid; CCL, C-C motif chemokine ligand; CX3CR1, C-X3-C motif chemokine receptor 1; CXCL, C-X-C motif chemokine ligand; FOLR/FRβ, folate receptor beta; gMFI, geometric mean fluorescence intensity; HDM, house dust mite; hMDMs, human monocyte-derived macrophages; HSPC, hematopoietic stem and progenitor cell; IL-9R, interleukin-9 receptor; ILC2s, group 2 innate lymphoid cells; IM, interstitial macrophage; MARCKS, myristoylated alanine-rich C-kinase substrate; M-CSF/CSF1, colony-stimulating factor 1; MertK, MER tyrosine kinase; moDCs, monocyte-derived dendritic cells; nor-NOHA, Nω-Hydroxy-nor-L-arginine; NSG, NOD scid gamma mouse strain; PBMC, peripheral blood mononuclear cell; PCA, Principal Component Analysis; T2, type 2 inflammation; Th2, T helper 2 cell; and t-SNE, t-distributed Stochastic Neighbor Embedding.

## INTRODUCTION

Macrophages are among the most abundant immune cells in the lung at homeostasis and play an important role in bridging innate and adaptive immune responses during disease development. Two functionally distinct macrophage populations, alveolar macrophages (AM) and interstitial macrophages (IM) are defined by their compartmentalization and surface receptor expression (1-3). CD43 (also known as leukosialin or sialophorin), a mucin-like glycoprotein, regulates adhesion, migration, and signaling and can serve as a broad marker to distinguish AMs from IMs (4-6). Macrophage populations are commonly identified by pan-macrophage markers including CD64, CD68, MertK, and F4/80 (mouse). Classical alveolar macrophages (AMs) reside directly in the alveoli in contact with the external environment, maintain high levels of self-proliferation from embryonic origins, and are distinctively characterized by high expression of CD11c and HLA-DR (human) or SiglecF (mouse). In contrast, tissue-resident interstitial macrophages (IMs) are localized within the parenchyma between the epithelium and vasculature to manage barrier immunity and tissue remodeling; these are immunophenotypically separated by their expression of CD206, CX3CR1, and Folate Receptor beta (FRβ). In contrast, tissue-resident interstitial macrophages (IMs) are localized within the parenchyma between the epithelium and vasculature to manage barrier immunity and tissue remodeling; these are immunophenotypically separated by their expression of CD206, CX3CR1, and Folate Receptor beta (1-3, 7-14). Furthermore, during active inflammation, monocyte-derived macrophages (MoDMacs) are rapidly recruited to the airways, transiently upregulating CD88 and CD169 during their differentiation kinetics (2, 7, 8, 15, 16). Humanized mouse models have also been used to characterize lung macrophages. Chakarov and colleagues identified two conserved monocyte-derived IM subpopulations defined by CD206 and CD169 in the humanized MISTRG mouse model (7). However, the spectrum of macrophages in human lungs is still not clearly delineated.

Interleukin-9 (IL-9) is a pleiotropic cytokine implicated in the pathogenesis of various diseases, including allergic inflammation (17). IL-9 mediates biological functions through the IL-9 receptor (IL-9R), a heterodimeric complex composed of a unique IL-9Rα chain and a common γ-chain shared with receptors for other cytokines such as IL-2 and IL-4 (18, 19). IL-9R is expressed on multiple cell types including activated T cells, ILC2s, memory B cells and mast cells (17, 20-25). IL-9/IL-9R signaling drives allergic inflammation by inducing chemokine production and promoting eosinophil recruitment (11–13). Elevated expression levels of *IL9* and *IL9R* have also been observed in patients with asthma (11, 12, 14). Moreover, IL-9 is associated with severe

asthmatic responses in a patient challenge model (26). However, the mechanistic contribution of IL-9 to human asthma is still not fully understood.

Alternatively-activated macrophages have been associated with allergic inflammation in patients and mouse models and have a defined gene expression profile that includes arginase 1 (Arg1) (27-31). Importantly, Arg1 expression correlates with disease in asthma patient samples (32-41). Using a chronic HDM challenge model, we previously demonstrated a critical role for IL-9-responsive macrophages in the development of allergic inflammation (3, 42). IL-9 function in macrophages was Arg1-dependent (3). Moreover, elevated expression of IL-9 was correlated with serum arginase activity and lung function in patients with asthma (3). However, it remains unclear whether IL-9 induces Arg1-expressing human macrophages in an allergic environment. In the current study, we analyzed bronchoalveolar lavage from control or asthmatic patients to define macrophage phenotypes. We further used humanized mice to examine the responses of human lung macrophages to IL-9 in vivo. These data demonstrate that human lung macrophages express IL-9R, respond to IL-9 in vivo through expansion and increased Arg1 expression, and that IL-9 induces polyamine metabolism in vivo. Together, these data indicate that an IL-9/macrophage/Arg1 pathway modifies the lung metabolite environment.

## MATERIALS AND METHODS

*Study design.*

The aim of this study was to characterize IL-9-responsive macrophages in human allergic inflammation, and to uncover the mechanisms of the development of IL-9-mediated allergic diseases. We used flow cytometry to characterize macrophage phenotypes in the airways and lung tissue of humanized mice and in the BAL of patient samples. We examined changes in phenotype of macrophages in humanized mice following administration of IL-9 in vivo. We compared macrophage phenotypes in control and asthmatic patient BAL. Finally, we correlated IL-9 and macrophage phenotypes with polyamine concentrations in BAL samples.

*Humanized mouse model.*

The quadruple transgenic NSG QUAD [NOD.Cg-Prkdc$^{scid}$ Il2rg$^{tm1Wjl}$ Tg(CMV-IL3,CSF2,KITLG)1Eav Tg(CSF1)3Sz/J, (NSG QUAD, Strain # 028657)] mice and the triple transgenic NSGS [NOD.Cg-Prkdc scid Il2rg tm1wjl Tg (CMV-IL-3,CSF2,KITLG)1Eav./MloySzJ, (stock no. 013062)] mice were purchased from The Jackson Laboratory (Bar Harbor, ME). NSG-QUAD mice were bred in-house by the Indiana University Melvin and Bren Simon Comprehensive Cancer Center In Vivo Therapeutics Core. All the mice were maintained in the specific pathogen free facility SPF animal facilities (ambient temperature 70–72 °F, humidity 50%, light/dark cycle 12/12 h). Mice were given ad libitum irradiated Teklad Uniprim Medicated Diet (Harlan Laboratories, Indianapolis, IN, TD 06596) and autoclaved, acidified water. All experiments were performed with the approval of the Indiana University Institutional Animal Care and Use Committee. NSG QUAD (NSG-Q) mice express human CSF1 [colony stimulating factor 1 (M-CSF)], human interleukin-3 (IL3; IL-3), human granulocyte/macrophage-stimulating factor (CSF2; GM-CSF), and human Steel factor (KITLG; SCF or SF) on the immunodeficient NSG (Stock No. 05557) background.

*Engraftment of human CD34+ hematopoietic stem and progenitor cells into NSG-QUAD/NSGS mice.*

Frozen Human CD34+ HSPCs were isolated from umbilical cord blood were obtained from StemCell Technologies. Cells were thawed and allowed to recover in cytokine-rich medium [StemSpan SFEM II (StemCell Technologies) supplemented with 100 ng/ml recombinant human SCF (Peprotech) for four hours prior to engraftment. All experiments were performed with the approval of the Indiana University Institutional Animal Care and Use Committee.

To enable human HSPC engraftment, 7 weeks old mice were sub-lethally irradiated with 100 cGy (JL Shepherd & Associates MARK I model 68A). Four hours later, mice were intravenously injected with 2 x $10^4$ human CD34+ HSPC cells. CD34 reconstituted mice were bled 8 weeks post-injection to assess human immune system engraftment and experiments were performed at 12 weeks post-injection. All the mice surpassed 50% human CD45+ immune cells (Fig Suppl 1).

*IL-9 injection model.*

Humanized mice were treated daily with 2 µg recombinant human IL-9 (Biolegend, 594404) intranasally for three days. Mice were euthanized 1 day after final intranasal challenge. Lungs were lavaged with cold PBS two times. BAL fluid was collected, and cells were centrifuged at 1500g for 5 minutes at 4°C for further surface staining. The supernatant was saved at −80°C for ELISA analysis. The rest of the lung tissue was digested in 0.5 mg/ml collagenase A (Roche) media for 1 hour at 37°C with rotation. After digestion, the lungs were filtered through mesh and red blood cells were lysed with ACK lysis buffer for 5 mins (Lonza). Cells were washed with FACS buffer and stained for macrophages and their cell markers. Total macrophages were identified as live CD64+ CD14- CD206+ HLA-DR+ cells.

*Patient samples.*

Adult asthmatic patients and controls were participants in a Program Project on severe asthma at Indiana University (PI – Ben Gaston, MD). All studies with human subjects and samples were performed with approval from the Indiana University Institutional Review Board and required informed consent from a parent or guardian. Bronchoscopies with bronchial biopsies, brushes, and bronchoalveolar lavage were performed using the Severe Asthma Research Program (SARP) protocol (43). Pediatric asthmatic patient BAL samples from 12 asthmatic children (≤18 years old) were collected as approved by the Institutional Review Board at the University of Virginia. Asthmatic children had diagnostic bronchoscopies clinically indicated by recurrent wheeze and severe asthma. Patients with hallmarks of type 2 inflammation including blood eosinophilia were included in this study. Characteristics of the subset of patients selected for the presence or absence of physician-diagnosed asthma for this study are listed in Supplementary Tables E1-E3.

Fresh BAL was centrifuged to isolate BAL cells and acellular supernatant. Flow cytometry studies were performed on fresh BAL cells. The acellular supernatant was stored at -80$^o$ for future batch protein analysis on all the samples.

*Flow cytometry.*

Single cell suspensions were stained with a fixable viability dye (eBioscience) and antibodies for surface markers for 30 min at 4 °C before fixation with 4% paraformaldehyde for 10 min dark at room temperature. After fixation, cells were permeabilized with permeabilization buffer (eBioscience) overnight at 4 °C, and then stained for intracellular transcription factors for 30 min at 4 °C. After intracellular staining, cells were washed with FACS buffer and analyzed by LSR4 or Fortessa (BD Biosciences) and analyzed with Flowjo 10.10 software (Tree Star). Reagents for flow cytometry are listed in Supplementary Table E4.

*Total polyamine assay.*

Supernatant of human BAL samples, cell culture medium or cell lysate of cultured hMDMs was assessed for total polyamines using total Polyamine Assay Kit (Abcam, Cambridge, United Kingdom) according to the manufacturer's directions. Samples were deproteinized and treated with the kit's Sample Clean-Up reagent to eliminate interfering metabolites. Samples and a serial dilution of a polyamine standard were incubated with a selective enzyme mix, which generates hydrogen peroxide in the presence of polyamines. Following the addition of a fluorometric probe, the reaction was incubated at 37°C for 60 minutes protected from light. The fluorescence was measured at an excitation/emission of 535/587 nm using a FilterMax F5 multi-mode microplate reader (Molecular Devices).

*IL-9 enzyme-linked immunosorbent assay (ELISA).*

IL-9 ELISA (Biolegend) was performed according to the manufacturer's instruction. Briefly, 96-well plate was coated with antibody overnight at 4 °C. After washing 3 times with the wash buffer, 300 µl ELISA buffer was added to the plate and incubate at room temperature for 2 h. After washing 3 times with washing buffer, 100 µl samples were added to the plate and incubated at room temperature for 2 h. After washing three times, 100 µl diluted detection antibody was added to the plate and incubated at room temperature for 1 h. After washing the plate three times, 100 µl of diluted Avidin-HRP solution was added to the plate and incubated at room temperature for 30 min at dark. After washing the plate 3 times, 100 µl substrate was added to the plate. Plates were read at absorbance of 450 and 570 nm. The minimum detectable concentration of IL-9 for this ELISA set is 2 pg/ml.

*Hydroxyproline Assay.*

Supernatant of human BAL samples and cell lysate of cultured hMDMs were assessed for total hydroxyproline using total *Hydroxyproline Assay* Kit (Sigma-Aldrich, MAK459) according to the manufacturer's directions. Samples and standards were prepared in technical duplicates. Samples were hydrolyzed in 12 M HCl at 120 °C for 3 hours, evaporated, and reconstituted. Hydroxyproline standards and sample aliquots were added to a 96-well plate. Following the addition of Oxidation Buffer and Chloramine T Concentrate, plates were incubated at room temperature. Perchloric acid/isopropanol and DMAB Concentrate were then added. After color development, absorbance was measured at 560 nm.

*Human monocyte-derived macrophages (hMDMs) culture and treatment.*

Fresh peripheral blood mononuclear cells (PBMC) were counted and cultured in DMEM (Dulbecco's Modified Eagle Medium) containing 10% FBS, 1% Pen/strep, and 50ng/ml human M-CSF (BioLegend, 574805) for 5 days. On day 5, hMDMs were treated with 5 ng/mL human IL-4 (R&D systems, 202-IL) for 24 hours. hMDMs were treated with 20 ng/mL human IL-9 (Biolegend, 594404) in the presence or absence of 100 µM of Nω-Hydroxy-nor-L-arginine diacetate Salt (nor-NOHA, Sigma-Aldrich, 399275-1MG). Culture media was collected 24 hours later and stored at −80 °C or directly used for ELISA assays. Cells were lysed and protein were extracted and stored at −80 °C or directly used for ELISA assays.

*Cell sorting and bulk RNA sequencing*.

Human BAL CD43- and CD43+ macrophages were sorted using a FACSAria or SORPAria cell sorter (BD Biosciences). The following gating strategies were applied: live $CD64^+$ $HLA\text{-}DR^+$ $CD43^{-/+}$. BAL cells from 3 patients were pooled together prior to sorting and staining. Immediately following sorting, RNA was extracted using the RNeasy Micro kit (Qiagen, 74004) according to the manufacturer's instructions. The quality and quantity of purified RNA was determined using Agilent Bioanalyzer 2100. A total of 1 ng of RNA per sample was used for library preparation. cDNA synthesis was performed using the SMART-Seq v4 Ultra Low Input RNA Kit for Sequencing (Takara Clontech Laboratories, Inc.). Dual-indexed cDNA libraries were then constructed using the Nextera XT DNA Library Prep Kit (Illumina, Inc.). Library concentration and quality were assessed using a Qubit Fluorometer and an Agilent Bioanalyzer, respectively, and libraries were pooled at equimolar concentrations. Pooled libraries were denatured and neutralized before loading onto a NovaSeq X PLUS sequencer (Illumina, Inc.) for 100 bp paired-end sequencing. Each library generated approximately 50–70 million reads.

*Analysis of Bulk RNA sequencing*

Sequencing reads were quality-checked using FastQC (v0.11.5). High-quality reads were aligned to the human reference genome using the STAR aligner (v2.7.10a). Mapping quality and read distribution across annotated genomic regions were evaluated using bamUtils (v0.4.17). Uniquely mapped reads were assigned to RefGene features using featureCounts (Subread v2.0.3), filtering out low-quality alignments from downstream analyses. Transcript abundance was quantified from raw sequencing reads using Salmon to generate transcript-level expression estimates. Transcript-level quantification data were subsequently imported and summarized to the gene level using the tximport package in R (v4.3.2), utilizing the org.Hs.eg.db package to map Ensembl transcript identifiers to official human gene symbols. Differential gene expression analysis between experimental macrophage groups was performed using the DESeq2 package, utilizing a generalized linear model based on the negative binomial distribution. High-dimensional data relationships were assessed via Principal Component Analysis (PCA) applied to regularized log-transformed (*rlog*) counts.

Transcript-level quantification data were subsequently imported and summarized to the gene level using the tximport package in R (v4.3.2), utilizing the org.Hs.eg.db package to map Ensembl transcript identifiers to official human gene symbols. Differential gene expression analysis between experimental macrophage groups was performed using the DESeq2 package, utilizing a generalized linear model based on the negative binomial distribution. High-dimensional data relationships were assessed via Principal Component Analysis (PCA) applied to regularized log-transformed (rlog) counts. Statistical thresholds for significance were set at an adjusted p value $< 0.05$ and an absolute $\log_2$ fold-change $> 1$. FASTQ files are available at GSE338526.

*Statistics analysis.*

Statistics were analyzed using GraphPad Prism V10 (GraphPad Software) and presented as means ± SEM. Nonparametric Mann-Whitney Student t tests and/or one-way ANOVA analysis were used in data analysis. Significance is indicated as follows: *, $p < 0.05$; **, $p < 0.01$; ***, $p < 0.001$; ****, $p < 0.0001$.

## RESULTS

*CD43 expression distinguishes two macrophage populations in lung and BAL of patients and NSG-Quad humanized mice.* Although our previous studies supported a role for macrophage in murine allergic airway disease (3), we wanted to verify these finding and determine if these observations were present in patients. To define macrophage populations in the lung of humanized mice, we compared macrophage development in humanized mouse models using NSGS mice (expressing human KitL, IL-3 and SCF) and NSG QUAD mice (expressing human KitL, IL-3, SCF, and M-CSF). NSG QUAD or NSGS mice that received 100cGy at the age of week 7 to delete bone marrow, were then transplanted with 2 x $10^4$ human CD34 cells (Fig 1A, s1A). Chimerism was analyzed in peripheral blood at 15 weeks of age, 8 weeks after engraftment (Fig. E1B). Both NSGS and NSG Quad mice in our study developed greater than 60% hCD45+ immune cells in periphery blood (Fig E1B, C). Macrophages were analyzed using a gating strategy shown on Fig. 1B. Compared to NSGS mice, we observed a much higher percentage of CD64+ HLA-DR+ CD206+ CD14- macrophages in BAL and lung from NSG-Quad mice (Fig E1D, E). This is consistent with other studies that NSG-Quad mice supported the development of macrophages.

A panel of macrophage markers was used to analyze cells in the BAL and lung tissue. Based on a recent study from Evran et al which demonstrated that alveolar, interstitial and intravascular macrophages in MISTRG humanized mice are CD206 positive (1, 44), we gated on CD64+ CD14- cells and identified macrophages as CD206+ and HLA-DR+. We then used CD43 (sialophorin, leukosialin), CD169 (Siglec1), CD88 (C5aR), FOLR (FRβ), CD11c and MARCKS (myristoylated alanine-rich C-kinase substrate) to define sub-populations of macrophages (3-6, 13, 14, 44-50). The expression level of cell markers was analyzed by using t-SNE analysis of macrophages (Fig 1C, D). Two macrophage subpopulations were distinguishable based on the presence or absence of CD43 expression. The CD43- subset expressed higher MARCKS, but lower CD11c and FOLR (Fig 1C, D). Further histogram analysis also showed that CD43- macrophages had higher expression of CD169, CD88 and MARCKS, but less expression of CD11c and FOLR in cells from the lung (Fig 1E). BAL CD43- and CD43+ macrophages had expression of these markers that paralleled lung tissue (Fig 1F).

To further investigate the macrophage subsets during lung inflammation in human subjects, we collected BAL samples from 6 adult asthmatic (mean age, 23.3 years, 3 males and 3 females) and 5 healthy control (mean age, 36.2 years, 2 males and 3 females) patients according to procedures approved by Indiana University (Supplementary Table E1). A similar

gating strategy was used to define subsets of macrophages in human BAL (Fig 2A). As in humanized mice, CD43 expression distinguished two macrophage subpopulations (Fig 2B). However, the CD43- population had lower CD169 and CD88 but higher CX3CR1 and MARCKS expression, which differed from the humanized mouse model (Fig. 2B-C). When compared to healthy control patients, the BAL cells from asthmatic patients had a higher percentage of macrophages and a lower percentage of CD43+, CD169+ macrophages compared to healthy control patients. The macrophages from asthmatic patients had higher percentages of CX3CR1+ and CD11c+ cells (Fig 2D). Together, these data indicate that humanized mice parallel but are not identical to patient BAL cells, and that there are changes in the proportions of some macrophage populations in patients with asthma.

*Expansion of CD43- macrophages following IL-9 treatment.* To directly evaluate the effects of IL-9 on human lung macrophages, we treated NSG-Quad humanized mice with daily recombinant human IL-9 (2 µg) *intranasally* for three days. Mice were euthanized 1 day after the final *intranasal* challenge. IL-9 treatment did not alter the percentage or total number of human macrophages (CD64+ CD14- HLA-DR+ CD206+) in the lung (Fig 3A). We observed a dramatic increase in the percentage and total number of CD43- macrophages, with a corresponding decrease of CD43+ macrophage percentages (Fig 3B, C). We similarly observed a significant increase in total macrophage numbers in BAL of IL-9-treated humanized mice (Fig 3D) and there was a dramatic increase in percentages and total numbers of the CD43- population, and a corresponding decrease of CD43+ macrophage percentages (Fig 3E, F). The differences in macrophage populations between control and asthmatic patients paralleled what we observed with IL-9 treatment of humanized mice. We found that BAL samples from asthmatic patients had higher percentage of macrophages (Fig. 2D) and a higher percentage of CD43- macrophages with a lower percentage of CD43+ macrophages compared to BAL samples from healthy control patients (Fig. 3G). Thus, IL-9 promotes the expansion of CD43- macrophages in the lung of a humanized mouse model, and these changes are reflected in a similar increase of CD43- macrophages in asthma patient BAL samples, compared to healthy controls.

*The IL-9R/Arg1 axis in lung macrophages.* Our previous study showed that macrophages are IL-9-responsive cells that are essential for allergic inflammation in the lung and IL-9 impacted the function of lung macrophages by inducing Arg1 activity in a chronic lung inflammation mouse model of HDM challenge (3). We also observed IL-9R expression on human monocytes and a correlation between concentrations of IL-9 and chemokines in patient samples (3). Our results showed that more Arg1+ cells were defined in asthmatic adults and Arg1 was higher in BAL cells

from IL-9 treated humanized NSGS-QUAD mice (Fig E2A-C). The majority of the Arg1+ cells were CD64+ HLA-DR+ macrophages in human BAL samples and in both lung and BAL cells of humanized mice (Fig E2D-F). Furthermore, more CD64+ HLA-DR+ macrophages were defined in asthmatic adults (Fig E2D).

To directly test the impact of IL-9 on human macrophages, we isolated lung and BAL cells from humanized mice following IL-9 intranasal treatment. IL-9R was expressed on, and Arg1 was expressed in, CD43- and CD43+ macrophages. In cells isolated from lung, the expression of IL-9R and Arg1 was higher in the CD43- macrophage population than in CD43+ macrophages (Fig 4A). We observed higher expression of Arg1 but similar IL-9R expression in CD43- macrophages compared to CD43+ macrophages from the BAL (Fig 4B). IL-9 treatment increased both IL-9R and Arg1 expression in the CD43- subpopulation assessed as percentage and cell numbers of positive cells (Fig 4C, D). In BAL cells, we observed similar findings that IL-9 treatment increased both IL-9R+ and Arg1+ percentages and cell numbers of CD43- macrophages (Fig 4E, F). This provides further evidence that an IL-9/macrophage/Arg1 axis exists in human macrophages and suggests that dynamic regulation of IL-9R may change the intrinsic ability of macrophage subpopulations to respond to IL-9. IL-9 treatment also increased the percent positive and/or cell number positive for other markers including CD88, CD11c and CX3CR1 in CD43- macrophages from freshly isolated lung or BAL cells (Fig E3A, B).

We further defined IL-9R and Arg1 expression of CD43- and CD43+ macrophages in BAL from asthmatic patients compared to cells from healthy control patients. Both IL-9R and Arg1 were expressed at a similar level in CD43- and CD43+ macrophages in human BAL samples and higher expression compared to healthy controls (Fig 5A, B). Other cell markers analysis by flow cytometry showed that there was a higher percentage of CX3CR1 and CD11c expression on CD43- macrophages in asthmatic BAL samples (Fig E3C).

To expand these observations into a pediatric population, we collected BAL samples from 12 asthmatic children (≤18 years old) at the University of Virginia. BAL samples were collected from 6 asthmatic children with type 2-low inflammation (mean age, 9.3 years, 4 males and 2 females) and 6 asthmatic children with type 2-high inflammation (mean age, 10.6 years, 4 males and 2 females) according to procedures approved by University of Virginia (Supplementary Table E3). Asthmatic children had diagnostic bronchoscopies clinically indicated by recurrent wheeze and severe asthma. We observed a significant increase in percentages of the CD43- macrophage population of BAL samples from T2-high asthmatic children compared to T2-low asthmatic children (Fig E4A). We also observed similar results from BAL cells with higher expression of IL-

9R and Arg1 on CD43- macrophages from T2-high asthmatic children compared to T2-low asthmatic children (Fig E4B). We further compared BAL cells from asthmatic adults and T2-high asthmatic children. The BAL samples from asthmatic children had less expansion of macrophages but had similar increases of CD43- and decreases of CD43+ macrophage populations (Fig 6A). The expression of IL-9R on, and Arg1 in, CD43- or CD43+ macrophages from adult and pediatric asthmatic samples were similarly increased in either, compared to healthy adult controls (Fig 6B, C). Pediatric asthmatic samples had similar expression levels of other macrophage markers comparable to those observed in adults (Fig E4D).

To understand how airway macrophages change their transcriptional signatures in the context of allergic inflammation, we performed bulk RNA sequencing using flow-sorted CD43- and CD43+ human BAL macrophages from healthy control and asthmatic patients. Principal Component Analysis (PCA) indicated the CD43- macrophage samples from asthmatic patients were distinct from the CD43- macrophages of healthy control patients, and both were separated from the CD43+ macrophage populations that clustered together (Fig 7A). We also observed a profound transcriptional response unique to the CD43- macrophages during asthma, which accounted for 4,225 up-regulated and 585 down-regulated differentially expressed genes (DEGs) compared to controls. However, only a small fraction of genes was altered in CD43+ macrophages when comparing asthmatic samples to control (Fig 7B, C). Asthmatic samples had broader impact on the upregulated genes compared to healthy control samples (Fig. E5A). Focusing on the differential expression between the two negative cohorts, the group-mean expression profile heatmap for priority genes reveals a stark divergence. The asthmatic group exhibits a strong upregulation of several key immune and inflammatory genes—including chemokines like *CCL18, CCL23, CCL24,* and *CXCL9*, as well as *MARCKS* and *C5AR1*—paired with the upregulation of transcription factors such as *CEBPB, MAF*, and *MAFB*. Conversely, the control cohort displays a distinct signature characterized by the upregulation of a smaller subset of genes, most notably *IKBKG* and *TLR7*, highlighting a distinct molecular shift in macrophage activation and signaling between healthy controls and asthmatic states (Fig 7D, E5B-D). These data indicate the important role of CD43- macrophages of IL-9R signaling during allergic inflammation.

*The polyamine pathway in the allergic lung.* Arg1 catabolizes L-arginine to L-ornithine, which is the rate limiting metabolite for polyamine production (31, 51, 52). We analyzed IL-9 and polyamine concentration in adult human patients BALF samples; asthmatic patients had significantly greater concentrations of polyamines and IL-9 than healthy controls (Fig 8A). IL-9

concentration in BALF was also positively correlated to polyamine concentration and the percentage of CD43- macrophages in human BAL (Fig. 8B). Moreover, BALF polyamine concentrations were positively correlated to the percentage of CD43- macrophages as well as subpopulations positive for IL-9R or Arg1 (Fig 8C, E6A). Similarly, there were increased concentrations of IL-9 and polyamines in the BALF of T2-high patients compared to T2-low patients and these were correlated to percentages of CD43- macrophages (Fig 8D, E). BALF polyamine levels were also positively correlated to the percentage of IL-9R+, Arg1+, and CD43- macrophages (Fig 8F, E6B).

In humanized mice, IL-9 treatment increased polyamine concentrations in BALF and the increase of polyamines was positively correlated to the percentage of CD43- macrophages (Fig. 8G-I, s6C). The increase of polyamines was also positively correlated to the percentage of IL-9R+ and Arg1+ CD43- macrophages (Fig 8I). There were higher hydroxyproline concentrations in asthmatic adult patient BALF than in healthy control patient samples (Fig 8J). We also did not observe significant differences in IL-9 concentrations in patient serum from adults or children, suggesting the IL-9/macrophage pathway is local and not systemic (Fig E6D, E).

To directly test the ability of IL-9 to modify arginase activity and polyamine production from human macrophages, we cultured hMDMs with or without IL-9 and with or without the arginase inhibitor, nor-NOHA. nor-NOHA is a potent, selective, and reversible arginase inhibitor of L-arginine breakdown. IL-9 stimulation increased percentages of CD43- hMDMs and the expression of Arg1 in both CD43- and CD43+ hMDMs (Fig 8K, E6F-H). The increase of Arg1 expression of hMDMs was blocked by nor-NOHA addition (Fig 8K, E6G, H). The IL-9-induced increase of polyamines in macrophages and culture media, increased arginase activity of macrophages and the increase of hydroxyproline in cells were blocked by nor-NOHA addition (Fig 8 L, M). This indicates that the synthesis of polyamines in macrophages is arginase-dependent. Collectively, these data suggest that IL-9 contributes to allergic airway inflammation by increasing the expression of IL-9R and Arg1 of CD43- macrophages and polyamines in the lung environment.

DISCUSSION

The results in this report further support the role of IL-9 in modulating macrophage function in the lung. IL-9 expands macrophage populations in both mouse models and in humanized mice and there is a similar expansion of macrophages in asthmatic BAL, compared to healthy control BAL. IL-9 also upregulates expression of its own receptor (IL-9R) and of the target gene Arg1 in human lung macrophages, and similar changes are observed in asthmatic patients, compared to controls. This is consistent with significantly increased IL-9 concentrations in asthmatic vs. control BAL. Finally, asthmatic patient BAL had higher polyamine concentrations that correlated with IL-9 concentrations and IL-9R+/Arg1+ macrophages. IL-9 induced polyamine concentrations in the humanized mouse BAL, further supporting the model that IL-9 promotes polyamine metabolism in macrophages. Mechanistically, using the selective arginase inhibitor nor-NOHA, we demonstrated that IL-9-induced polyamine metabolism in macrophages is Arg1-dependent. Together, these data support a model in which IL-9/macrophage/polyamine axis is a metabolically active engine driving airway inflammation and remodeling.

Macrophages in our study were defined as CD64+ HLA-DR+ CD206+ CD14- cells, a stringent gating strategy that effectively excludes classical monocyte-derived dendritic cells (moDCs) and other intravascular monocytes, all of which typically have low or absent expression of CD206 (1, 49, 53-55). We further took advantage of CD43, a hematopoietic cell antigen whose distribution includes T lymphocytes, monocytes, macrophages, plasma cells, neutrophils, and platelets and was described as a differential marker mediating macrophage trafficking and phagocytosis (6, 45-48, 50). CD43 has been shown to distinguish AMs (CD43+) from IMs (CD43-) (4-6). Our present data showed that CD64+ HLA-DR+ CD206+ macrophages in lung can be easily distinguished into two subsets, CD43- and CD43+ macrophages. Under homeostatic conditions, interstitial macrophages (IMs) are localized tightly within the tissue parenchyma. However, during active airway inflammation, monocyte-derived IM-like populations are actively recruited into the alveolar space and can be recovered via BAL (11, 56). This explains why the marked shift in the CD43- macrophage population following IL-9 treatment was restricted predominantly to the BAL compartment rather than the lung tissue parenchyma.

We noted an interesting immunophenotypic discrepancy between patient samples and humanized mice; while CD169 was higher on CD43+ than CD43- macrophages from patient samples, humanized mice had more homogenous expression of CD169. The lack of distinction of CD169 between CD43- and CD43+ populations may result from the short time of human CD34+ immune cells engraftment, and that this population is derived from monocytes during the

engraftment. In the humanized NSG-Quad model, tissue-resident populations including CD43- interstitial-like macrophages are actively derived from circulating blood monocytes. This rapid differentiation under acute human cytokine support may explain the transient retention or upregulation of CD169. In contrast, human clinical BAL samples reflect a chronic, long-term inflammatory milieu where mature IM sub-populations have undergone extensive microenvironmental priming, matching established single-cell human lung atlases that define classical human IMs as CD206+ CD169-. Importantly, despite these baseline differences in surface marker density, the core functional and transcriptional responses of the CD43- population remain conserved between model and patient. In BAL cells from asthmatic or healthy control subjects, the CD43- macrophages have less expression of CD169 compared to CD43+ macrophages. This indicates that CD43- macrophages may be similar to interstitial macrophages (IM), defined as CD206+ CD169- cells in Evren et al (1), while CD43+ macrophages are predominantly CD206+ CD169+ AMs. Our data showed that CD43- macrophages from lung and BAL of IL-9-treated humanized mice model have greater expression of CX3CR1, MARCKS and lower FOLR. This suggests that these two separated populations of macrophages are functionally different and that the greater CX3CR1 expression on CD43- macrophages in BAL from asthmatic patients and from lung and BAL cells of IL-9-treated humanized mice play distinct functional roles during lung inflammation. Monocytes and macrophages are known to migrate in a CCL2/CCR2 axis during allergic airway inflammation (3, 57), and our previous study found that IL-9 regulated classical monocyte migration to the lung via CCR2 (3). As CX3CR1 plays a significant role in lung inflammation by mediating leukocyte adhesion and migration within the lung tissue (10), our observations suggest that CX3CR1 might be contributing to the movement of interstitial macrophages.

Humanized mouse models, defined as immunodeficient mice engrafted with a human immune system, have provided valuable information for human-specific studies. Reconstitution of the human immune system is achieved by transplantation of human CD34+ hematopoietic stem and progenitor cells (HSPCs) into immunodeficient mice (1, 58, 59). There are several humanized mouse models developed to investigate human myeloid cell lineages. MISTRG-6 mice support the development and function of human monocytes, macrophages, and natural killer (NK) cells, including infiltration of human melanoma xenografts by human macrophages (1, 58, 60). Quadruple transgenic NSG-Quad mice support human CD33+ and CD14+ cell development and can be engrafted with human-induced pluripotent stem cells (61, 62). We compared NSGS mice and NSG-Quad mice models for the development of human myeloid cell lineages and gated macrophages as CD64+ CD14- HLA-DR+ CD206+. CD14- was used to exclude circulating blood

monocytes and recently migrated cells. NSG-Quad mice developed much greater numbers and proportions of human macrophages in freshly isolated lung and BAL cells compared to NSGS mice. Recently, a study also compared NSG-Quad and MISTRG mice for modeling circulating and tumor-infiltrating human myeloid cells (58). NSG-Quad mice supported the development of varying human myeloid cell lineages and promoted the development of tissue-resident as well as tumor-infiltrating human CD68+ macrophages at a level comparable to MISTRG-6 mice. However, the development of NK cells, CD4+ T cells, and CD8+ T cells in NSG-Quad mice was reduced compared to MISTRG-6 mice (58). Thus, while humanized mouse models have structural limitations, they reflect the differing environmental complexities between a controlled, short-term human hematopoietic stem cell engraftment model and the chronic, multi-lineage inflammatory environment found in patients.

IL-9 is known to enhance type 2 immune responses in allergic diseases (17), with mast cells being direct IL-9-responsive cells in asthma (25, 63, 64). Additional studies have implicated IL-9 in the functions of multiple cell types, including Th2 cells, epithelial cells and B cells (20, 24, 25). However, knowledge about IL-9-targeted cells is still limited. Our previous study assessed IL-9R expression across various cell types to identify IL-9-responsive populations in allergic airway inflammation with mice model defined the lung macrophages occupied a significant proportion of the IL-9R+ cells. They also express relatively high amounts of IL-9R compared to other cell types, such as eosinophils and neutrophils (3). Interstitial macrophages mediated IL-9-dependent allergic responses and IL-9 affected the function of lung macrophages by inducing Arg1 activity (3). Moreover, IL-9R expression was detected in human blood monocytes and alveolar macrophages (65, 66). However, IL-9 regulation of lung macrophages in disease states is still poorly understood, especially in humans. Our data uncovers a previously unappreciated target, the CD43- macrophage population, that acts as a key component for IL-9-mediated allergic responses by increasing Arg1 activity and polyamine production. RNA-seq data demonstrates a distinct transcriptional upregulation of core inflammatory chemokines (including *CCL18, CCL23*, and *CCL24*) specifically in human asthmatic CD43- macrophages. This reinforces our previous findings in murine systems (3). Although this study has advanced the understanding of IL-9-responsive macrophages in the allergic environment, further studies are required to investigate the transition from monocytes to macrophages in various microenvironments, their biological functions in specific inflammatory responses, and their transcriptional programs.

Arg1 is an important enzyme that regulates macrophage functions (67) and is a marker of macrophage alternative activation. Our previous study demonstrated that Arg1 in macrophages

is clearly required for the development of chronic lung inflammation in an HDM model (3). Pro-allergic function is consistent with other studies, as well as patient samples where increased Arg1 expression and arginase activity are associated with progressive asthma development (38-41). The stimuli for Arg1 expression in lung macrophages during disease is still not clear. Previous studies have shown that IL-4 and IL-13 can induce Arg1 expression and promote an immunosuppressive macrophage phenotype (67). In this present study, we demonstrated that macrophages are the majority of Arg1+ cells in human BAL cells and lung and BAL cells from humanized mice. Arg1 expression in human macrophages and arginase activity is clearly increased in response to IL-9 in a humanized mouse model and consistent with our data collected from human BAL samples from eosinophilic asthmatic patients. Together, these observations suggest that the function of Arg1 in the lung may be a major effector of IL-9/IL-9R pathway. Increased Arg1 may modulate the allergic environment by increasing the production of polyamines by catabolizing arginine to ornithine, a primary substrate that feeds into polyamine metabolism (68). Polyamines had been well characterized in M2 macrophage responses to various parasitic and fungal infections (69-72) and recent studies found that polyamines regulate M1 macrophage activation and mucosal inflammation (72, 73). Although the synthesis of polyamines can theoretically occur via agmatine pathways and polyamines can enter a cell through direct transport machinery independent of arginase (74), our functional cultured human macrophage perturbation experiments utilizing the arginase inhibitor nor-NOHA nearly abolished the IL-9-mediated increase in polyamines in both cell lysates and culture supernatants. This indicates that in human airway macrophages, this specific cytokine-driven pathway is predominantly arginase-dependent. Furthermore, the polyamine pathway potentially links to airway tissue remodeling and collagen deposition, supported by the IL-9-dependent induction of hydroxyproline. IL-9 directly induces a significant accumulation of hydroxyproline (a key proxy for extracellular matrix deposition) in human macrophages, which is halted by arginase inhibition. In our present study, higher levels of polyamines in BALF of humanized mice and human asthmatic patients were positively correlated to BALF IL-9 concentration and increased IL-9R+ and Arg1+ CD43- macrophages. Collectively, these data suggest that the IL-9R/Arg1 pathway promotes polyamine metabolism in human airway macrophages.

The clinical implications of using anti-IL-9 antibody treatments have been substantiated in preclinical mouse models (63, 75-78) and human trials (79-81). Despite the modest therapeutic outcomes observed across heterogeneous patient populations, these findings underscore the potential of precision immunology. Specifically, identifying IL-9–high patient phenotypes may enable more precise application of IL-9 blockade stratifying with meaningful clinical impact (82).

Our present report demonstrates that the IL-9R/Arg1/polyamine axis is conserved between adult and pediatric asthma patients, further supporting its role as a fundamental, generalized driver of allergic airway inflammation. Therefore, targeted therapeutic strategies to block the IL-9/macrophage/polyamine axis in lung macrophages offers a possible approach for treating asthma and potentially other pulmonary inflammatory diseases.

ACKNOWLEDGMENTS

*Funding:*

This work is supported by Public Health Service grants from the National Institutes of Health (R01 AI129241 and R01 AI180518 to M.H.K.; P01HL158507 to B.G., H.L.T. and K.M.K.). NIH AI147394, AG069264, AI112844, HL170961, AI176171 and AG090337 to J.S., American Lung Association Catalyst Grant to I.S.C. The Indiana University Melvin and Bren Simon Comprehensive Cancer Center In Vivo Therapeutics Core & Flow Cytometry Resource Facility are funded in part by NIH, National Cancer Institute (NCI) grant P30 CA082709 and National Institute of Diabetes and Digestive and Kidney Diseases (NIDDK) grant U54 DK106846. The FCRF is supported in part by NIH instrumentation grant 1S10D012270. Support provided by the Herman B Wells Center for Pediatric Research is, in part, from the Riley Children's Foundation.

References

1. Evren E, Ringqvist E, Tripathi KP, Sleiers N, Rives IC, Alisjahbana A, et al. Distinct developmental pathways from blood monocytes generate human lung macrophage diversity. Immunity. 2021;54(2):259-75.e7.
2. Hussell T, Bell TJ. Alveolar macrophages: plasticity in a tissue-specific context. Nature reviews Immunology. 2014;14(2):81-93.
3. Fu Y, Wang J, Zhou B, Pajulas A, Gao H, Ramdas B, et al. An IL-9-pulmonary macrophage axis defines the allergic lung inflammatory environment. Science immunology. 2022;7(68):eabi9768.
4. Venosa A, Malaviya R, Choi H, Gow AJ, Laskin JD, Laskin DL. Characterization of Distinct Macrophage Subpopulations during Nitrogen Mustard-Induced Lung Injury and Fibrosis. American journal of respiratory cell and molecular biology. 2016;54(3):436-46.
5. Gibbings SL, Jakubzick CV. A Consistent Method to Identify and Isolate Mononuclear Phagocytes from Human Lung and Lymph Nodes. Methods Mol Biol. 2018;1799:381-95.
6. Hume PS, Gibbings SL, Jakubzick CV, Tuder RM, Curran-Everett D, Henson PM, et al. Localization of Macrophages in the Human Lung via Design-based Stereology. American journal of respiratory and critical care medicine. 2020;201(10):1209-17.
7. Chakarov S, Lim HY, Tan L, Lim SY, See P, Lum J, et al. Two distinct interstitial macrophage populations coexist across tissues in specific subtissular niches. Science. 2019;363(6432).
8. Gibbings SL, Thomas SM, Atif SM, McCubbrey AL, Desch AN, Danhorn T, et al. Three Unique Interstitial Macrophages in the Murine Lung at Steady State. American journal of respiratory cell and molecular biology. 2017;57(1):66-76.
9. Schyns J, Bai Q, Ruscitti C, Radermecker C, De Schepper S, Chakarov S, et al. Non-classical tissue monocytes and two functionally distinct populations of interstitial macrophages populate the mouse lung. Nature communications. 2019;10(1):3964.
10. Moon HG, Kim SJ, Kim KH, Kim YM, Rehman J, Lee H, et al. CX(3)CR(1)(+) Macrophage Facilitates the Resolution of Allergic Lung Inflammation via Interacting CCL26. American journal of respiratory and critical care medicine. 2023;207(11):1451-63.
11. Aegerter H, Lambrecht BN, Jakubzick CV. Biology of lung macrophages in health and disease. Immunity. 2022;55(9):1564-80.
12. Han W, Zaynagetdinov R, Yull FE, Polosukhin VV, Gleaves LA, Tanjore H, et al. Molecular imaging of folate receptor β-positive macrophages during acute lung inflammation. American journal of respiratory cell and molecular biology. 2015;53(1):50-9.
13. Chen Z, Zhang W, Selmi C, Ridgway WM, Leung PSC, Zhang F, et al. The myristoylated alanine-rich C-kinase substrates (MARCKS): A membrane-anchored mediator of the cell function. Autoimmunity Reviews. 2021;20(11):102942.
14. Issara-Amphorn J, Sjoelund VH, Smelkinson M, Montalvo S, Yoon SH, Manes NP, et al. Myristoylated, alanine-rich C-kinase substrate (MARCKS) regulates toll-like receptor 4 signaling in macrophages. Scientific reports. 2023;13(1):19562.
15. Abdul Qayum A, Koh B, Martin RK, Kenworthy BT, Kharwadkar R, Fu Y, et al. The Il9 CNS-25 Regulatory Element Controls Mast Cell and Basophil IL-9 Production. J Immunol. 2019;203(5):1111-21.
16. Epelman S, Lavine KJ, Randolph GJ. Origin and functions of tissue macrophages. Immunity. 2014;41(1):21-35.
17. Kaplan MH, Hufford MM, Olson MR. The development and in vivo function of T helper 9 cells. Nat Rev Immunol. 2015;15(5):295-307.
18. Kimura Y, Takeshita T, Kondo M, Ishii N, Nakamura M, Van Snick J, et al. Sharing of the IL-2 receptor gamma chain with the functional IL-9 receptor complex. International immunology. 1995;7(1):115-20.

19. Russell SM, Johnston JA, Noguchi M, Kawamura M, Bacon CM, Friedmann M, et al. Interaction of IL-2Rb and gc chains with Jak1 and Jak 3: Implications for XSCID and XCID. Science. 1994;266:1042-5.
20. Takatsuka S, Yamada H, Haniuda K, Saruwatari H, Ichihashi M, Renauld JC, et al. IL-9 receptor signaling in memory B cells regulates humoral recall responses. Nature immunology. 2018;19(9):1025-34.
21. Wilhelm C, Hirota K, Stieglitz B, Van Snick J, Tolaini M, Lahl K, et al. An IL-9 fate reporter demonstrates the induction of an innate IL-9 response in lung inflammation. Nature immunology. 2011;12(11):1071-7.
22. Nowak EC, Weaver CT, Turner H, Begum-Haque S, Becher B, Schreiner B, et al. IL-9 as a mediator of Th17-driven inflammatory disease. The Journal of experimental medicine. 2009;206:1653-60.
23. Elyaman W, Bradshaw EM, Uyttenhove C, Dardalhon V, Awasthi A, Imitola J, et al. IL-9 induces differentiation of TH17 cells and enhances function of FoxP3+ natural regulatory T cells. Proceedings of the National Academy of Sciences of the United States of America. 2009;106:12885-90.
24. Wang Y, Shi J, Yan J, Xiao Z, Hou X, Lu P, et al. Germinal-center development of memory B cells driven by IL-9 from follicular helper T cells. Nature immunology. 2017;18(8):921-30.
25. Sehra S, Yao W, Nguyen ET, Glosson-Byers NL, Akhtar N, Zhou B, et al. TH9 cells are required for tissue mast cell accumulation during allergic inflammation. J Allergy Clin Immunol. 2015;136(2):433-40.e1.
26. Alladina J, Smith NP, Kooistra T, Slowikowski K, Kernin IJ, Deguine J, et al. A human model of asthma exacerbation reveals transcriptional programs and cell circuits specific to allergic asthma. Science immunology. 2023;8(83):eabq6352.
27. Abdelaziz MH, Abdelwahab SF, Wan J, Cai W, Huixuan W, Jianjun C, et al. Alternatively activated macrophages; a double-edged sword in allergic asthma. J Transl Med. 2020;18(1):58.
28. Byers DE, Holtzman MJ. Alternatively activated macrophages and airway disease. Chest. 2011;140(3):768-74.
29. Jang JC, Nair MG. Alternatively Activated Macrophages Revisited: New Insights into the Regulation of Immunity, Inflammation and Metabolic Function following Parasite Infection. Curr Immunol Rev. 2013;9(3):147-56.
30. Nair MG, Du Y, Perrigoue JG, Zaph C, Taylor JJ, Goldschmidt M, et al. Alternatively activated macrophage-derived RELM-{alpha} is a negative regulator of type 2 inflammation in the lung. The Journal of experimental medicine. 2009;206(4):937-52.
31. Pesce JT, Ramalingam TR, Mentink-Kane MM, Wilson MS, El Kasmi KC, Smith AM, et al. Arginase-1-expressing macrophages suppress Th2 cytokine-driven inflammation and fibrosis. PLoS pathogens. 2009;5(4):e1000371.
32. Meurs H, Zaagsma J, Maarsingh H, van Duin M. Recent Patents in Allergy/Immunology: Use of arginase inhibitors in the treatment of asthma and allergic rhinitis. Allergy. 2019;74(6):1206-8.
33. Morris CR, Poljakovic M, Lavrisha L, Machado L, Kuypers FA, Morris SM, Jr. Decreased arginine bioavailability and increased serum arginase activity in asthma. American journal of respiratory and critical care medicine. 2004;170(2):148-53.
34. Donthi S, Neela VSK, Gaddam S, Mohammed HH, Ansari SS, Valluri VL, et al. Association of increased risk of asthma with elevated arginase & interleukin-13 levels in serum & rs2781666 G/T genotype of arginase I. Indian J Med Res. 2018;148(2):159-68.
35. Duan QL, Gaume BR, Hawkins GA, Himes BE, Bleecker ER, Klanderman B, et al. Regulatory haplotypes in ARG1 are associated with altered bronchodilator response. American journal of respiratory and critical care medicine. 2011;183(4):449-54.

36. Kochanski L, Kossmann S, Rogala E, Dwornicki J. [Sputum arginase activity in bronchial asthma]. Pneumonol Pol. 1980;48(5):329-32.
37. Lara A, Khatri SB, Wang Z, Comhair SA, Xu W, Dweik RA, et al. Alterations of the arginine metabolome in asthma. American journal of respiratory and critical care medicine. 2008;178(7):673-81.
38. Litonjua AA, Lasky-Su J, Schneiter K, Tantisira KG, Lazarus R, Klanderman B, et al. ARG1 is a novel bronchodilator response gene: screening and replication in four asthma cohorts. American journal of respiratory and critical care medicine. 2008;178(7):688-94.
39. Cloots RH, Sankaranarayanan S, de Theije CC, Poynter ME, Terwindt E, van Dijk P, et al. Ablation of Arg1 in hematopoietic cells improves respiratory function of lung parenchyma, but not that of larger airways or inflammation in asthmatic mice. Am J Physiol Lung Cell Mol Physiol. 2013;305(5):L364-76.
40. Cloots RHE, Poynter ME, Terwindt E, Lamers WH, Kohler SE. Hypoargininemia exacerbates airway hyperresponsiveness in a mouse model of asthma. Respir Res. 2018;19(1):98.
41. Cloots RHE, Sankaranarayanan S, Poynter ME, Terwindt E, van Dijk P, Lamers WH, et al. Arginase 1 deletion in myeloid cells affects the inflammatory response in allergic asthma, but not lung mechanics, in female mice. BMC Pulm Med. 2017;17(1):158.
42. Fu Y, Pajulas A, Wang J, Zhou B, Cannon A, Cheung CCL, et al. Mouse pulmonary interstitial macrophages mediate the pro-tumorigenic effects of IL-9. Nature communications. 2022;13(1):3811.
43. Moore WC, Evans MD, Bleecker ER, Busse WW, Calhoun WJ, Castro M, et al. Safety of investigative bronchoscopy in the Severe Asthma Research Program. J Allergy Clin Immunol. 2011;128(2):328-36.e3.
44. Ural BB, Yeung ST, Damani-Yokota P, Devlin JC, de Vries M, Vera-Licona P, et al. Identification of a nerve-associated, lung-resident interstitial macrophage subset with distinct localization and immunoregulatory properties. Science immunology. 2020;5(45).
45. Chung J, Vallurupalli M, Noel S, Schor G, Liu Y, Nobrega C, et al. Sialylated CD43 is a glyco-immune checkpoint for macrophage phagocytosis. bioRxiv. 2025.
46. Howell DN, Ahuja V, Jones L, Blow O, Sanfilippo FP. Differential expression of CD43 (leukosialin, sialophorin) by mononuclear phagocyte populations. Journal of leukocyte biology. 1994;55(4):536-44.
47. Randhawa AK, Ziltener HJ, Merzaban JS, Stokes RW. CD43 is required for optimal growth inhibition of Mycobacterium tuberculosis in macrophages and in mice. J Immunol. 2005;175(3):1805-12.
48. Schiefermeier-Mach N, Haller T, Geley S, Perkhofer S. Migrating Lung Monocytes Internalize and Inhibit Growth of Aspergillus fumigatus Conidia. Pathogens. 2020;9(12).
49. Singleton H, Graham SP, Bodman-Smith KB, Frossard JP, Steinbach F. Establishing Porcine Monocyte-Derived Macrophage and Dendritic Cell Systems for Studying the Interaction with PRRSV-1. Front Microbiol. 2016;7:832.
50. Venosa A, Malaviya R, Gow AJ, Hall L, Laskin JD, Laskin DL. Protective role of spleen-derived macrophages in lung inflammation, injury, and fibrosis induced by nitrogen mustard. Am J Physiol Lung Cell Mol Physiol. 2015;309(12):L1487-98.
51. Canè S, Geiger R, Bronte V. The roles of arginases and arginine in immunity. Nature reviews Immunology. 2025;25(4):266-84.
52. Herbert DR, Orekov T, Roloson A, Ilies M, Perkins C, O'Brien W, et al. Arginase I suppresses IL-12/IL-23p40-driven intestinal inflammation during acute schistosomiasis. J Immunol. 2010;184(11):6438-46.
53. Desch AN, Gibbings SL, Goyal R, Kolde R, Bednarek J, Bruno T, et al. Flow Cytometric Analysis of Mononuclear Phagocytes in Nondiseased Human Lung and Lung-Draining Lymph Nodes. American journal of respiratory and critical care medicine. 2016;193(6):614-26.

54. Bharat A, Bhorade SM, Morales-Nebreda L, McQuattie-Pimentel AC, Soberanes S, Ridge K, et al. Flow Cytometry Reveals Similarities Between Lung Macrophages in Humans and Mice. American journal of respiratory cell and molecular biology. 2016;54(1):147-9.
55. Jakubzick C, Gautier EL, Gibbings SL, Sojka DK, Schlitzer A, Johnson TE, et al. Minimal differentiation of classical monocytes as they survey steady-state tissues and transport antigen to lymph nodes. Immunity. 2013;39(3):599-610.
56. Johnston LK, Rims CR, Gill SE, McGuire JK, Manicone AM. Pulmonary macrophage subpopulations in the induction and resolution of acute lung injury. American journal of respiratory cell and molecular biology. 2012;47(4):417-26.
57. Lee YG, Jeong JJ, Nyenhuis S, Berdyshev E, Chung S, Ranjan R, et al. Recruited alveolar macrophages, in response to airway epithelial-derived monocyte chemoattractant protein 1/CCl2, regulate airway inflammation and remodeling in allergic asthma. American journal of respiratory cell and molecular biology. 2015;52(6):772-84.
58. Chen A, Knöbl V, Walzer O, Hauser J, Neuwirth I, Frank M, et al. Comparison of NSG-Quad and MISTRG-6 humanized mice for modeling circulating and tumor-infiltrating human myeloid cells. Mol Ther Methods Clin Dev. 2025;33(2):101487.
59. Chuprin J, Buettner H, Seedhom MO, Greiner DL, Keck JG, Ishikawa F, et al. Humanized mouse models for immuno-oncology research. Nature Reviews Clinical Oncology. 2023;20(3):192-206.
60. Rongvaux A, Willinger T, Martinek J, Strowig T, Gearty SV, Teichmann LL, et al. Development and function of human innate immune cells in a humanized mouse model. Nat Biotechnol. 2014;32(4):364-72.
61. Shultz LD, Keck J, Burzenski L, Jangalwe S, Vaidya S, Greiner DL, et al. Humanized mouse models of immunological diseases and precision medicine. Mamm Genome. 2019;30(5-6):123-42.
62. Svoboda DS, Barrasa MI, Shu J, Rietjens R, Zhang S, Mitalipova M, et al. Human iPSC-derived microglia assume a primary microglia-like state after transplantation into the neonatal mouse brain. Proceedings of the National Academy of Sciences of the United States of America. 2019;116(50):25293-303.
63. Kearley J, Erjefalt JS, Andersson C, Benjamin E, Jones CP, Robichaud A, et al. IL-9 governs allergen-induced mast cell numbers in the lung and chronic remodeling of the airways. American journal of respiratory and critical care medicine. 2011;183(7):865-75.
64. Pajulas A, Fu Y, Cheung CCL, Chu M, Cannon A, Alakhras N, et al. Interleukin-9 promotes mast cell progenitor proliferation and CCR2-dependent mast cell migration in allergic airway inflammation. Mucosal immunology. 2023.
65. Pilette C, Ouadrhiri Y, Van Snick J, Renauld JC, Staquet P, Vaerman JP, et al. IL-9 inhibits oxidative burst and TNF-alpha release in lipopolysaccharide-stimulated human monocytes through TGF-beta. J Immunol. 2002;168(8):4103-11.
66. Donninelli G, Saraf-Sinik I, Mazziotti V, Capone A, Grasso MG, Battistini L, et al. Interleukin-9 regulates macrophage activation in the progressive multiple sclerosis brain. Journal of neuroinflammation. 2020;17(1):149.
67. Murray PJ. Macrophage Polarization. Annu Rev Physiol. 2017;79:541-66.
68. Hesse M, Modolell M, La Flamme AC, Schito M, Fuentes JM, Cheever AW, et al. Differential regulation of nitric oxide synthase-2 and arginase-1 by type 1/type 2 cytokines in vivo: granulomatous pathology is shaped by the pattern of L-arginine metabolism. J Immunol. 2001;167(11):6533-44.
69. Liao CP, Lasbury ME, Wang SH, Zhang C, Durant PJ, Murakami Y, et al. Pneumocystis mediates overexpression of antizyme inhibitor resulting in increased polyamine levels and apoptosis in alveolar macrophages. The Journal of biological chemistry. 2009;284(12):8174-84.

70. Seabra SH, DaMatta RA, de Mello FG, de Souza W. Endogenous polyamine levels in macrophages is sufficient to support growth of Toxoplasma gondii. J Parasitol. 2004;90(3):455-60.
71. Heby O, Persson L, Rentala M. Targeting the polyamine biosynthetic enzymes: a promising approach to therapy of African sleeping sickness, Chagas' disease, and leishmaniasis. Amino Acids. 2007;33(2):359-66.
72. Hardbower DM, Asim M, Luis PB, Singh K, Barry DP, Yang C, et al. Ornithine decarboxylase regulates M1 macrophage activation and mucosal inflammation via histone modifications. Proceedings of the National Academy of Sciences of the United States of America. 2017;114(5):E751-E60.
73. Puleston DJ, Buck MD, Klein Geltink RI, Kyle RL, Caputa G, O'Sullivan D, et al. Polyamines and eIF5A Hypusination Modulate Mitochondrial Respiration and Macrophage Activation. Cell metabolism. 2019;30(2):352-63 e8.
74. Van den Bossche J, Lamers WH, Koehler ES, Geuns JM, Alhonen L, Uimari A, et al. Pivotal Advance: Arginase-1-independent polyamine production stimulates the expression of IL-4-induced alternatively activated macrophage markers while inhibiting LPS-induced expression of inflammatory genes. Journal of leukocyte biology. 2012;91(5):685-99.
75. Cheng G, Arima M, Honda K, Hirata H, Eda F, Yoshida N, et al. Anti-interleukin-9 antibody treatment inhibits airway inflammation and hyperreactivity in mouse asthma model. American journal of respiratory and critical care medicine. 2002;166(3):409-16.
76. Kim MS, Cho KA, Cho YJ, Woo SY. Effects of interleukin-9 blockade on chronic airway inflammation in murine asthma models. Allergy Asthma Immunol Res. 2013;5(4):197-206.
77. Kung TT, Luo B, Crawley Y, Garlisi CG, Devito K, Minnicozzi M, et al. Effect of anti-mIL-9 antibody on the development of pulmonary inflammation and airway hyperresponsiveness in allergic mice. American journal of respiratory cell and molecular biology. 2001;25(5):600-5.
78. Arras M, Huaux F, Vink A, Delos M, Coutelier JP, Many MC, et al. Interleukin-9 reduces lung fibrosis and type 2 immune polarization induced by silica particles in a murine model. American journal of respiratory cell and molecular biology. 2001;24(4):368-75.
79. Oh CK, Leigh R, McLaurin KK, Kim K, Hultquist M, Molfino NA. A randomized, controlled trial to evaluate the effect of an anti-interleukin-9 monoclonal antibody in adults with uncontrolled asthma. Respir Res. 2013;14(1):93.
80. Parker JM, Oh CK, LaForce C, Miller SD, Pearlman DS, Le C, et al. Safety profile and clinical activity of multiple subcutaneous doses of MEDI-528, a humanized anti-interleukin-9 monoclonal antibody, in two randomized phase 2a studies in subjects with asthma. BMC Pulm Med. 2011;11:14.
81. White B, Leon F, White W, Robbie G. Two first-in-human, open-label, phase I dose-escalation safety trials of MEDI-528, a monoclonal antibody against interleukin-9, in healthy adult volunteers. Clin Ther. 2009;31(4):728-40.
82. Bick F, Blanchetot C, Lambrecht BN, Schuijs MJ. A reappraisal of IL-9 in inflammation and cancer. Mucosal immunology. 2025;18(1):1-15.

FIGURE LEGENDS

Figure 1. Macrophages from BAL and lung cells of humanized NSG-Quad mice had two distinguished CD43- and CD43+ subsets and had different other cell markers expressions. (A), Schematic of humanized NSG-Quad mouse model. (B), Gating strategy of CD64+ CD206+ HLA-DR+ macrophages from humanized mice. (C), t-SNE analysis of lung macrophages from humanized mice. (D), t-SNE analysis of BAL macrophages from humanized mice. (E), Histogram analysis of lung macrophages from humanized mice. (F), Histogram analysis of BAL macrophages from humanized mice.

Figure 2. Macrophages from BAL samples of adult asthmatic patients and healthy controls. (A), Gating strategy of CD64+ CD206+ HLA-DR+ macrophages from human BAL cells. (B), t-SNE analysis of BAL macrophages from human patients. (C), Histogram analysis of BAL macrophages from human patients. (D), Flow cytometry analysis of BAL macrophages from human patients for cell markers (n=5 Ctl; n=6 Asthmatic). *, $p<0.05$; **, $p<0.01$.

Figure 3. CD43- macrophage population expanded in response to IL-9 in humanized mice and in human BAL from asthmatic patients. (A), CD64+ CD206+ HLA-DR+ lung macrophages from humanized mice (% & #; n=10 PBS & IL-9). (B), Typical flow and t-SNE analysis of CD64+ CD206+ HLA-DR+ macrophages of lung from humanized mice. (C), CD43 subpopulations of CD64+ CD206+ HLA-DR+ lung macrophages from humanized mice (% & #; n=10 PBS & IL-9). (D), CD64+ CD206+ HLA-DR+ BAL macrophages from humanized mice (% & #; n=10 PBS & IL-9). (E), Typical flow and t-SNE analysis of CD64+ CD206+ HLA-DR+ BAL macrophages from humanized mice. (F), CD43 subpopulations of CD206+ HLA-DR+ BAL macrophages from humanized mice (% & #; n=10 PBS & IL-9). (G), Typical flow analysis of CD64+ CD206+ HLA-DR+ BAL macrophages from human asthmatic patients and healthy control person. And CD43 subpopulations of CD206+ HLA-DR+ BAL macrophages from human BAL samples (%; n=5 Ctl; n=6 Asthmatic). *, $p<0.05$; **, $p<0.01$; ***, $p<0.001$.

Figure 4. CD43- macrophages of IL-9 treated humanized mice had higher expression of IL-9R and Arg1. (A, B), t-SNE analysis and histogram analysis of lung and BAL macrophages from humanized mice for IL-9R and Arg1. (C, D), IL-9Ra expression of CD206+ HLA-DR+ macrophages of lung and BAL (% & #; n=10 PBS & IL-9). (E, F), Arg1 expression of CD206+

HLA-DR+ macrophages of lung and BAL (% & #; n=10 PBS & IL-9). *, p<0.05; **, p<0.01; ***, p<0.001; ****, p<0.0001.

Figure 5. CD43- macrophages of asthmatic patients had higher expression of IL-9R and Arg1. (A), Flow analysis of human BAL macrophages from asthmatic patients or healthy control persons. IL-9R expression of CD206+ HLA-DR+ macrophages (%; n=5 Ctl; n=6 Asthmatic). (B), Flow analysis of human BAL macrophages from asthmatic patients or healthy control persons. Arg1 expression of CD206+ HLA-DR+ macrophages (%; n=5 Ctl; n=6 Asthmatic). *, p<0.05; **, p<0.01; ***, p<0.001; ****, p<0.0001.

Figure 6. The BAL samples from asthmatic children had less percentage of macrophages, but with similar percentage of CD43- and CD43+ percentage of subpopulations and their expression level of IL-9R and Arg1. (A), CD64+ HLA-DR+ CD206+ macrophages and CD43-, CD43+ macrophages (%; n=5 Healthy Ctl; n=6 Asthmatic Adults; n=6 Asthmatic Children). (B), IL-9R and Arg1 expression of CD43- and CD43+ macrophages (%; n=5 Healthy Ctl; n=6 Asthmatic Adults; n=6 Asthmatic Children). *, p<0.05; **, p<0.01; ***, p<0.001; ****, p<0.0001. Ordinary one-way ANOVA was used to generate P values.

Figure 7. CD43-/+ macrophages regulate transcription signature of macrophage pro-allergic functions. (A), PCA plots of $CD43^{-/+}$ macrophage clusters of adult asthmatic patients and healthy controls. (B), Venn diagram showing the number of overlapped upregulated genes between healthy control and asthmatic samples in CD43- and CD43+ macrophages. Top circle: CD43- macrophages Asthmatic vs Healthy Ctl; Bottom circle: CD43+ macrophages, Asthmatic vs Healthy Ctl; padj < 0.05, log2FC > 0.5. (C), Venn diagram showing the number of overlapped down-regulated genes between healthy control and asthmatic samples in macrophages. Top circle: CD43- macrophages Asthmatic vs Healthy Ctl; Bottom circle: CD43+ macrophages, Asthmatic vs Healthy Ctl; padj < 0.05, log2FC < -0.5. (D), Heatmap showing the average expression of selected overlapped genes in CD43- macrophages.

Figure 8. (A), BALF samples from adult asthmatic patients had higher level of polyamine, IL-9. n=5 Ctl; n=6 Asthmatic. (B), Correlation between IL-9 and polyamines of patient BALF and % CD43- macrophages of adults patient BAL. n=12. (C), Correlation between polyamine and % IL-9R+/Arg1+ CD43- macrophages of adults patient BAL. n=12. (D), BALF samples from T2 high children patients had higher levels of polyamine, IL-9 compared to T2 low patients. n=5 Ctl; n=6

Asthmatic. (E), Correlation between IL-9 and polyamines of children patient BALF and % CD43- macrophages of patient BAL. n=12. (F), Correlation between polyamine and % IL-9R+/Arg1+ CD43- macrophages of children patient BAL. n=12. (G), IL-9 treatment increased polyamine level in BALF supernatant of humanized NGS-QUAD mice. n=10 PBS & IL-9. (H), Correlation between polyamine and % CD43- macrophages of mouse BAL. n=20. (I), Correlation between polyamine and % IL-9R+/Arg1+ CD43- macrophages of mouse BAL. n=20. (J), Hydroxyproline concentration in adult patient BALF. n=12. . (K), % of IL-9R+ and Arg1+ macrophages of *in vitro* cultured hMDMs. n=4. (L), Arginase activity, polyamine concentration and hydroxyproline concentration of *in vitro* cultured hMDMs. n=4. (M), Polyamine concentration of culture medium. n=4. *, $p<0.05$; **, $p<0.01$; ***, $p<0.001$. Ordinary one-way ANOVA was used to generate P values of hMDMs data.

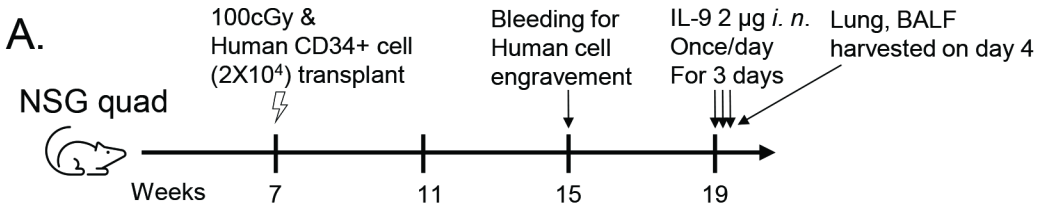


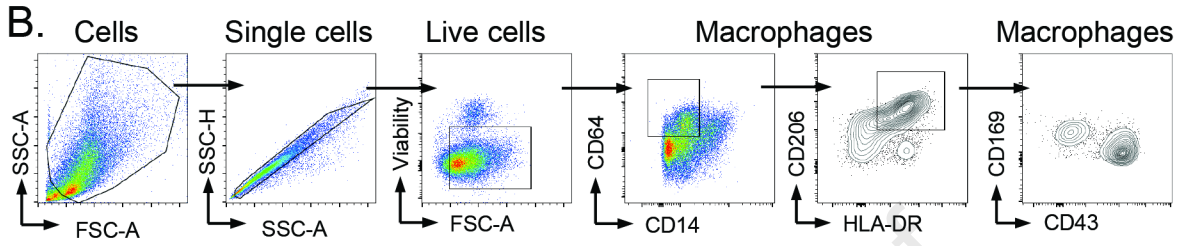


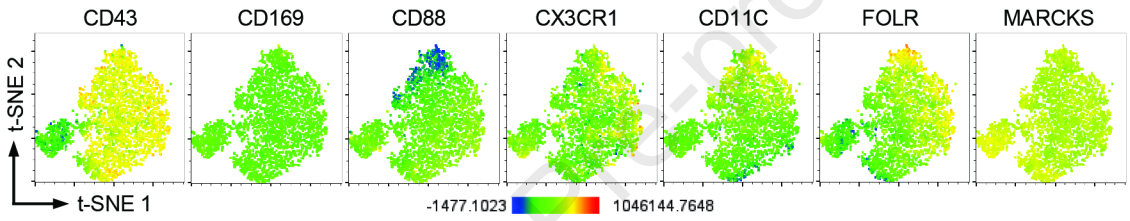


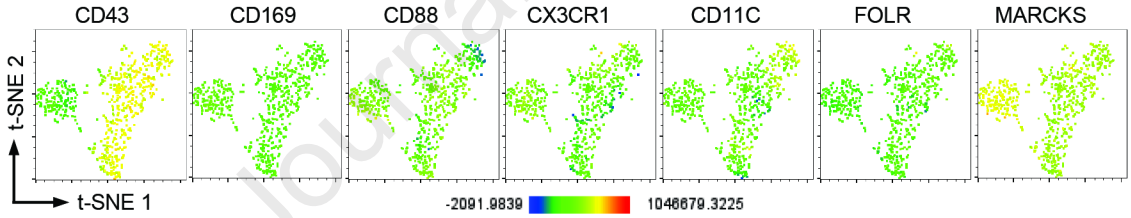


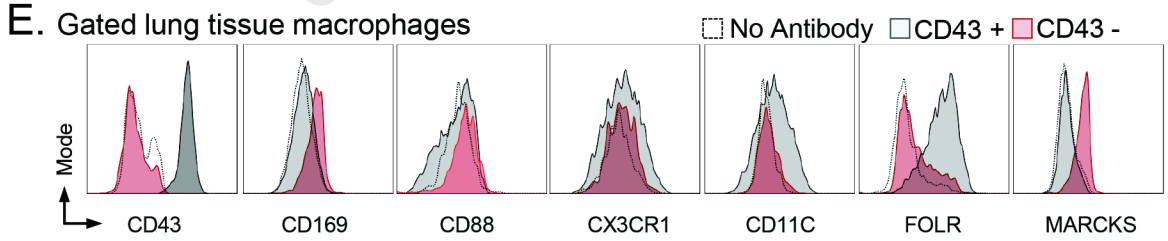


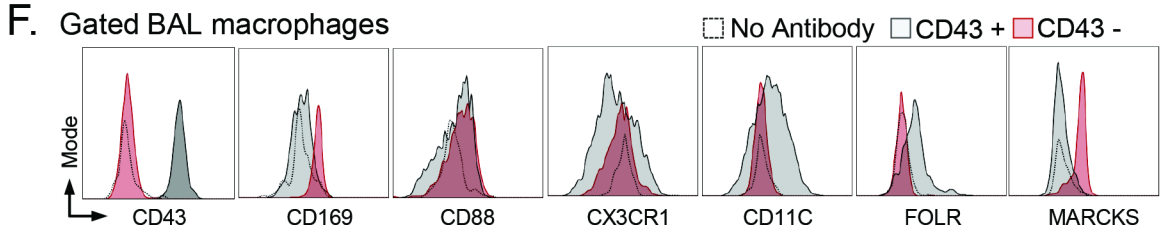

A.

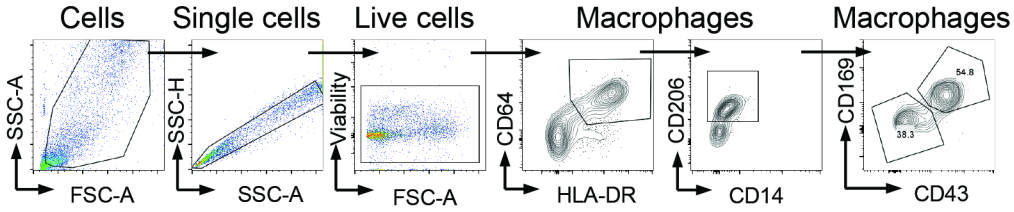


B. Gated human BAL macrophages

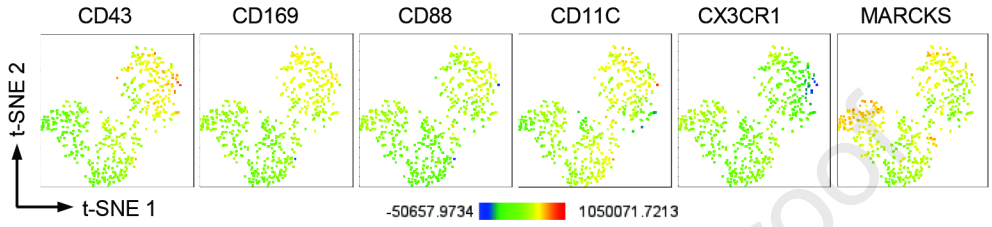


C. Gated human BAL macrophages

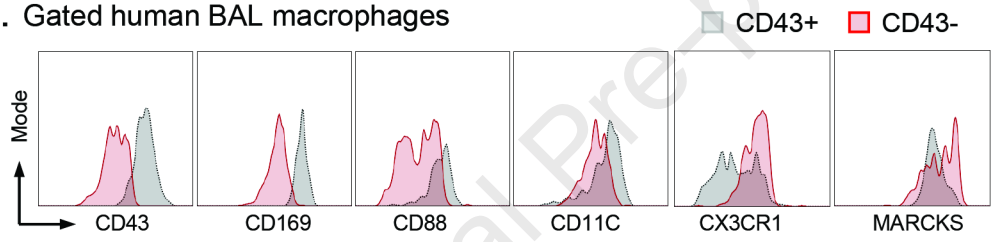


D. Human BAL macrophages

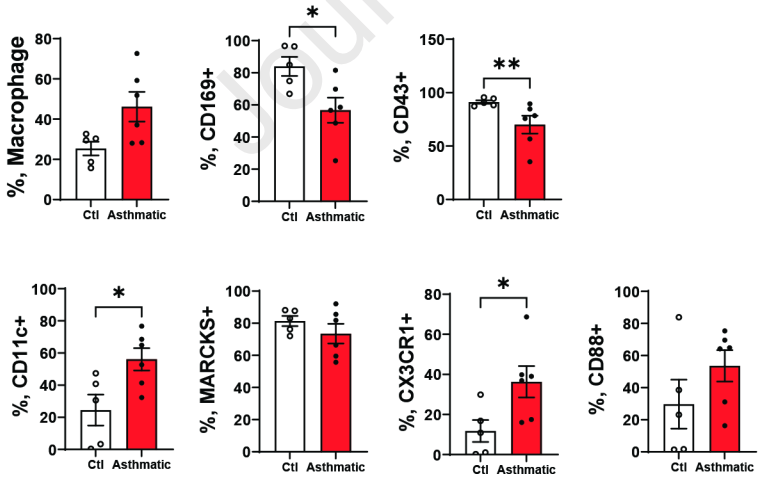

A. Lung of humanized mice

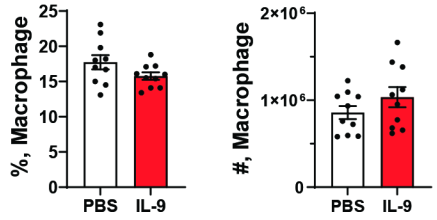


B. Gated lung tissue macrophages

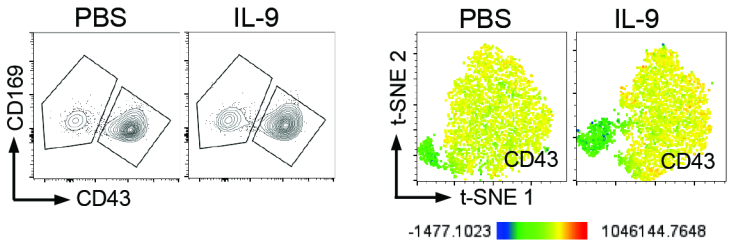


C. Gated lung tissue macrophages

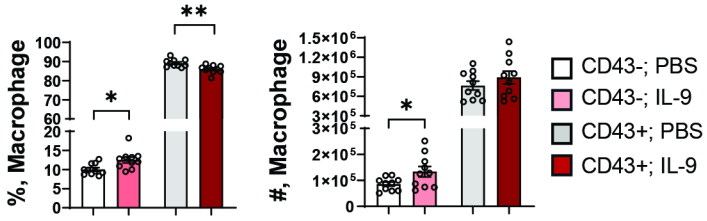


D. BAL of humanized mice

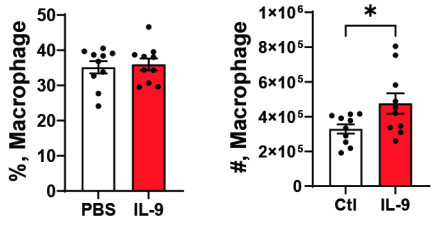


E. Gated BAL macrophages

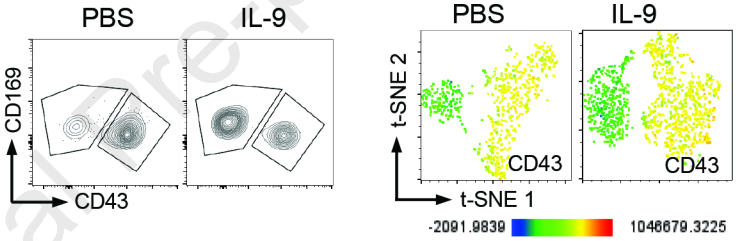


F. Gated BAL macrophages

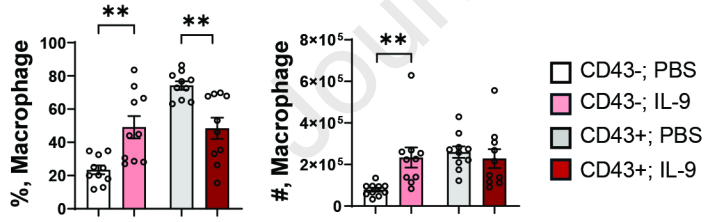


G. Gated human BAL macrophages

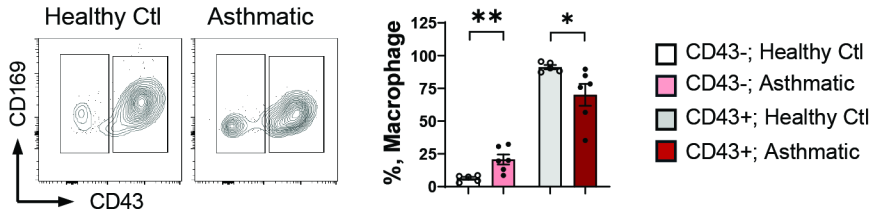

A. Gated lung tissue macrophages

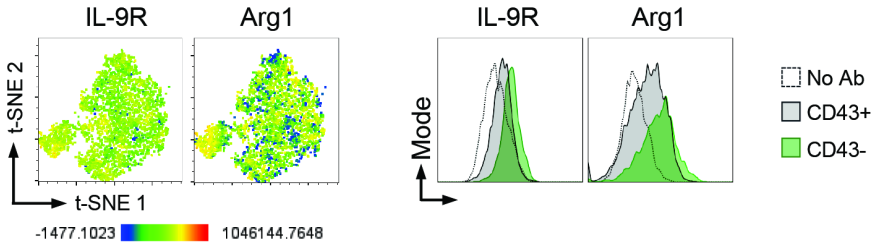


B. Gated BAL macrophages

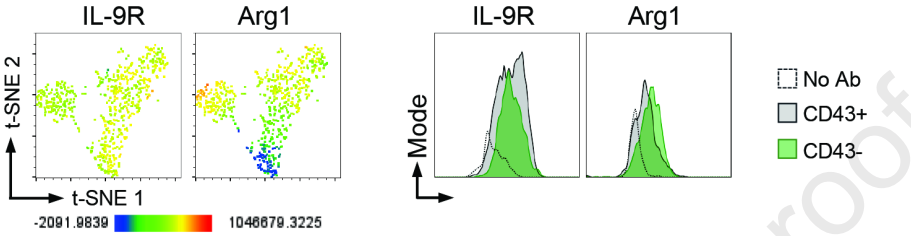


C. Gated lung tissue macrophages

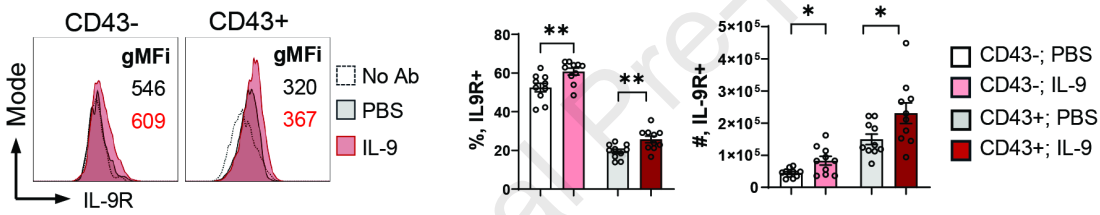


D. Gated lung tissue macrophages

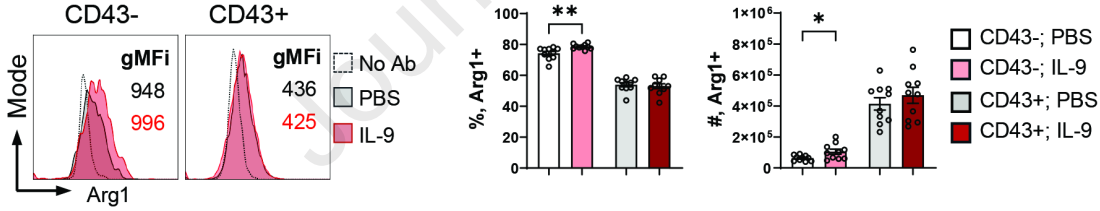


E. Gated BAL macrophages

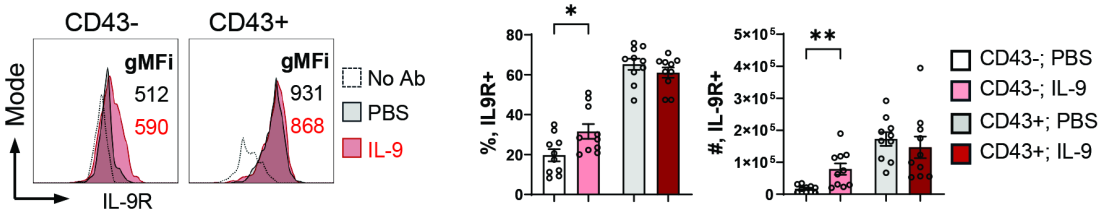


F. Gated BAL macrophages

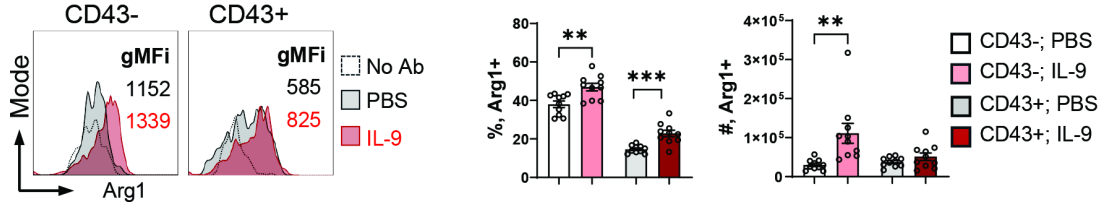

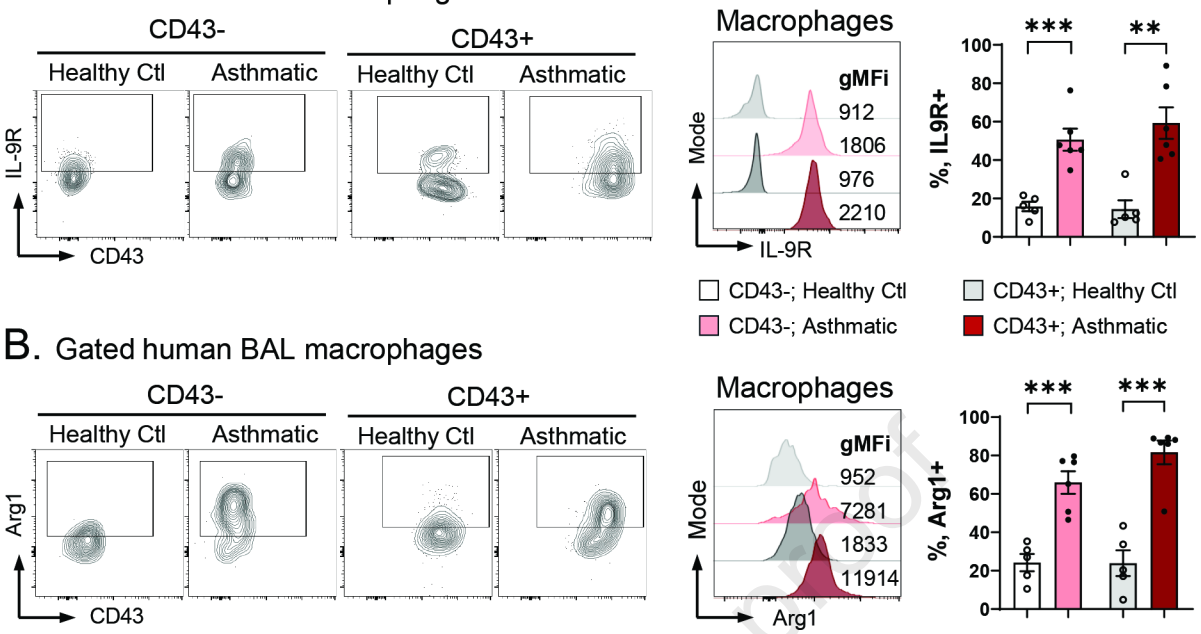

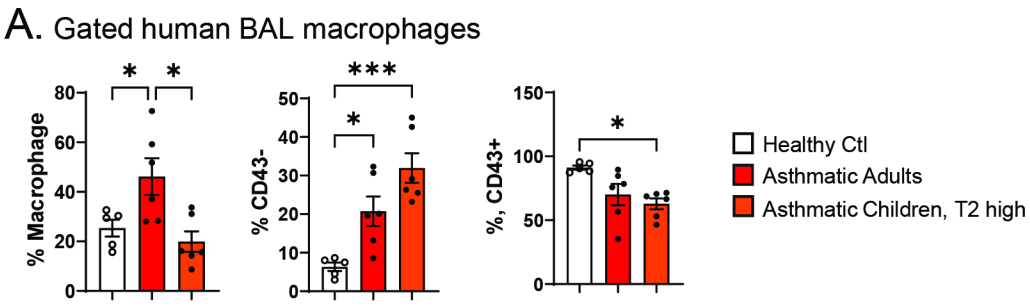


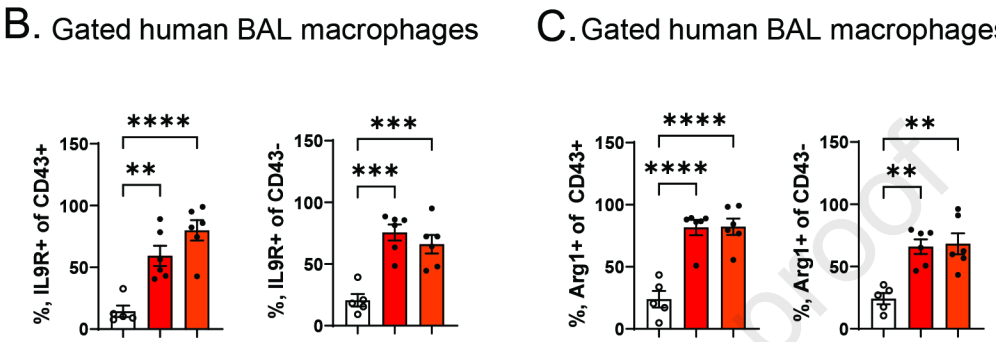

A.

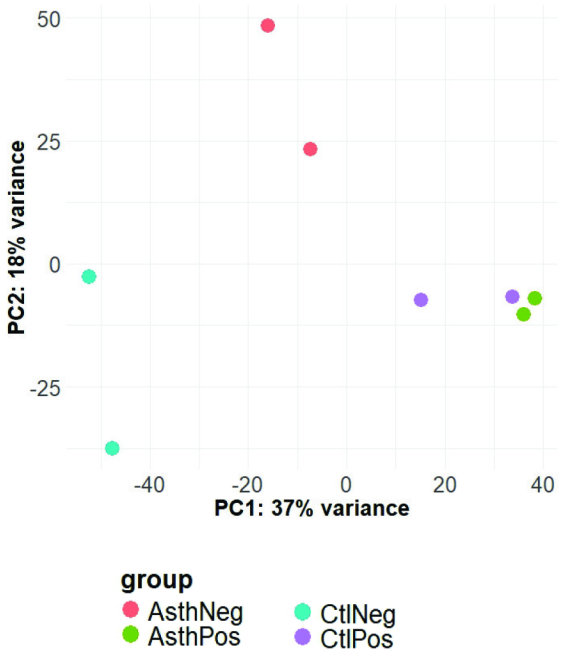


B.

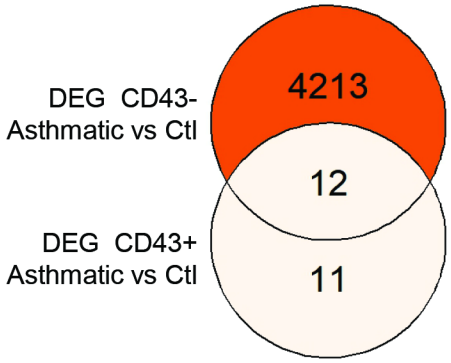


C.

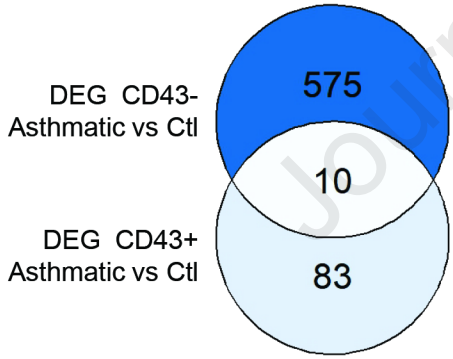


D. CD43- Macrophages